

Effects of minor Ca on as-cast microstructures and mechanical properties of Mg–3Ce–1.2Mn–0.9Sc and Mg–4Y–1.2Mn–0.9Sc alloys

Ming-bo YANG^{1,2,3}, Cheng-yu DUAN², De-yong WU², Fu-sheng PAN³

1. Key Laboratory of Manufacture and Test Techniques for Automobile Parts, Ministry of Education, Chongqing University of Technology, Chongqing 400054, China;

2. Materials Science and Engineering College, Chongqing University of Technology, Chongqing 400050, China;

3. National Engineering Research Center for Magnesium Alloys, Chongqing University, Chongqing 400030, China

Received 22 July 2013; accepted 19 October 2013

Abstract: The effects of the addition of 0.6% Ca (mass fraction) on the as-cast microstructure and mechanical properties of the Mg–3Ce–1.2Mn–0.9Sc and Mg–4Y–1.2Mn–0.9Sc magnesium alloys were investigated and compared by optical microscopy and scanning electron microscopy, differential scanning calorimetry analysis, and tensile and creep tests. The results indicate that the addition of 0.6% Ca to the Mg–3Ce–1.2Mn–0.9Sc and Mg–4Y–1.2Mn–0.9Sc alloys can refine the grains of the two alloys. At the same time, the addition of 0.6% Ca to the Mg–3Ce–1.2Mn–0.9Sc and Mg–4Y–1.2Mn–0.9Sc alloys can effectively improve the tensile properties of the two alloys. In addition, the addition of 0.6% Ca can also improve the creep properties of the Mg–3Ce–1.2Mn–0.9Sc alloy but is not beneficial to the creep properties of the Mg–4Y–1.2Mn–0.9Sc alloy. The different effects of minor Ca on the creep properties of the Mg–3Ce–1.2Mn–0.9Sc and Mg–4Y–1.2Mn–0.9Sc alloys are possibly related to the difference in the solid solubilities of Ce and Y in Mg.

Key words: magnesium alloys; Mg–RE–Mn–Sc alloys; Ca addition

1 Introduction

It is well known that the development of elevated temperatures magnesium alloys is very necessary to compete with other light constructional materials such as aluminum alloys. Previous investigations indicated that magnesium alloys based on Mg–Sc system exhibited interesting creep properties, and the additions of Mn, Ce and Y to Mg–Sc alloys could further improve the creep resistance [1,2]. Accordingly, the research and development on Mg–Ce/Y–Mn–Sc alloys have received many attentions and some positive results have been obtained [3–6]. It has been shown that the quaternary Mg–3Ce/4Y–1.2Mn–0.9Sc alloys are considerably superior to WE alloys (Mg–Y–Nd–Zr) and exhibit high creep resistance at high temperatures over 300 °C [4,7]. According to the investigations of MORDIKE et al [1], the high creep properties for the Mg–3Ce/4Y–1.2Mn–

0.9Sc alloys are mainly caused by the dense dispersion of fine Mn₂Sc particles. In addition, the grain boundary eutectic and the precipitation of Mg₁₂Ce possibly contribute to the further improvement of creep resistance for the Mg–3Ce–1.2Mn–0.9Sc alloy. As for the Mg–4Y–1.2Mn–0.9Sc alloy, the Mn- and Y-containing phase (Mn₁₂Y) parallel to *a*-Mg matrix basal planes and the stable Mg₂₄Y₅ phase at grain boundaries also possibly contribute to the further improvement of creep resistance.

Although the Mg–3Ce/4Y–1.2Mn–0.9Sc alloys are superior in creep resistance, they exhibit relatively low tensile properties, especially low ductility due to the coarse grains [3]. Further enhancement in the mechanical properties for the two alloys by grain refinement needs to be considered. In the previous investigations [8,9], it is found that minor Zr and/or Sr additions to the Mg–3Ce/4Y–1.2Mn–0.9Sc alloys can refine the grains, which leads to enhance the properties. However, it is not

Foundation item: Projects (CSTC2013jcyjC60001) supported by the Chongqing Science and Technology Commission of China; Project (KJ120834) supported by the Chongqing Education Commission of China; Project (CQUT1205) supported by the Open Funds from Key Laboratory of Manufacture and Test Techniques for Automobile Parts (Chongqing University of Technology), Ministry of Education, China

Corresponding author: Ming-bo YANG; Tel: +86-23-62563176; E-mail: yangmingbo@cqut.edu.cn

DOI: 10.1016/S1003-6326(14)63243-X

clear whether other additions such as Ca to the Mg–3Ce/4Y–1.2Mn–0.9Sc alloys have similar effects on the microstructures and properties as Zr and Sr additions. It is well known that Ca can behave as a grain refiner of magnesium alloys [10]. At the same time, JUN et al [11,12] and ZHANG et al [13] found that Ca addition to the Mg–RE alloys can not only refine the primary α -Mg grains but also increase the thermal stability of the Mg–RE phases in the alloys. Therefore, it is expected that Ca addition possibly plays a beneficial role in the grain refinement and mechanical properties for the Mg–3Ce/4Y–1.2Mn–0.9Sc alloys. Based on the above mentioned reasons, the present work investigates and compares the effects of minor Ca on the as-cast microstructure and mechanical properties of the Mg–3Ce–1.2Mn–0.9Sc and Mg–4Y–1.2Mn–0.9Sc magnesium alloys.

2 Experimental

The Ca-containing experimental alloys were prepared by adding pure Mg, Mg–29.24%Ce, Mg–17%Y, Mg–2.7%Sc, Mg–4.38%Mn, and/or Mg–19.7%Ca master alloys. The experimental alloys were melted in a crucible resistance furnace and protected by a flux addition. After being held at 740 °C for 20 min, the melts of the experimental alloys were respectively homogenized by mechanical stirring and then poured into a permanent mould which was coated and preheated to 200 °C in order to obtain a casting. The specimens whose size has been reported in Ref. [14] were fabricated from the casting for tensile and creep tests. Furthermore, the samples of the experimental alloys were subjected to a solution heat treatment (520 °C/12 h+water cooled) in order to reveal the grain boundaries and examine the microstructural stability at high temperatures. For comparison, the experimental alloys without Ca addition were also cast and machined into the same dimensions and tested under the same conditions as the above samples. Table 1 lists the actual chemical compositions of the experimental alloys, which were inspected by inductively coupled plasma spectroscopy.

Table 1 Actual compositions of experimental alloys (mass fraction, %)

Alloy	Composition/%					
	Ce	Y	Mn	Sc	Ca	Mg
Mg–3Ce–1.2Mn–0.9Sc	2.80	–	1.02	0.79	–	Bal.
Mg–3Ce–1.2Mn–0.9Sc–0.6Ca	2.78	–	1.12	0.81	0.49	Bal.
Mg–4Y–1.2Mn–0.9Sc	–	3.81	1.10	0.74	–	Bal.
Mg–4Y–1.2Mn–0.9Sc–0.6Ca	–	3.78	1.09	0.77	0.51	Bal.

In order to analyze the solidification behavior of the experimental alloys, the differential scanning calorimetry (DSC) was carried out using a NETZSCH STA 449C system equipped with platinum-rhodium crucibles. Samples of around 30 mg were heated in a flowing argon atmosphere from 30 to 700 °C for 5 min before being cooled down to 100 °C. The heating and cooling curves were recorded at a controlling speed of 15 °C/min.

The as-cast and solutionized samples of the experimental alloys were respectively etched in a 8% nitric acid solution in distilled water and a solution of 1.5 g picric, 25 mL ethanol, 5 mL acetic acid and 10 mL distilled water, and then examined by an Olympus optical microscope and/or JEOL JSM-6460LV type scanning electron microscope. The phases in the as-cast experimental alloys were also analyzed by D/Max-1200X type analyzer. The grain size was analyzed by the standard linear intercept method using an Olympus stereomicroscope. The tensile properties of the as-cast experimental alloys at room temperature and 300 °C were determined from a stress-strain curve, respectively. The ultimate tensile strength (UTS), 0.2% yield strength (YS), and elongation to failure were obtained based on the average value of three tests. The constant-load tensile creep tests were performed at 300 °C and 30 MPa for 100 h. The total creep strain and minimum creep rates of the as-cast experimental alloys were measured from each elongation versus time curve and averaged over three tests.

3 Results and discussion

3.1 Effects of minor Ca on as-cast microstructure

According to the XRD results of the as-cast alloys, the Mg–3Ce–1.2Mn–0.9Sc alloys with and without Ca addition are mainly composed of α -Mg, Mg₁₂Ce and Mn₂Sc phases, and the Mg–4Y–1.2Mn–0.9Sc alloys with and without Ca addition are mainly composed of α -Mg, Mg₂₄Y₅, Mn₁₂Y and Mn₂Sc phases. Obviously, the addition of 0.6% Ca to the Mg–3Ce/4Y–1.2Mn–0.9Sc alloys does not cause the formation of any new phases in the two alloys, which may be further confirmed from Fig. 1 which shows the DSC cooling curves of the as-cast alloys. As shown in Fig. 1, the DSC cooling curves of the as-cast alloys are similar, with two main peaks at about 630 and 570 °C, respectively, corresponding to the α -Mg matrix solidification and second phase transformations, which indicates that the addition of 0.6% Ca to the Mg–3Ce/4Y–1.2Mn–0.9Sc alloys does not influence the types of the phase transformations of the two alloys.

Figure 2 shows the optical images of the as-cast alloys. It is observed from Fig. 2 that the primary α -Mg phases in all the as-cast experimental alloys mainly

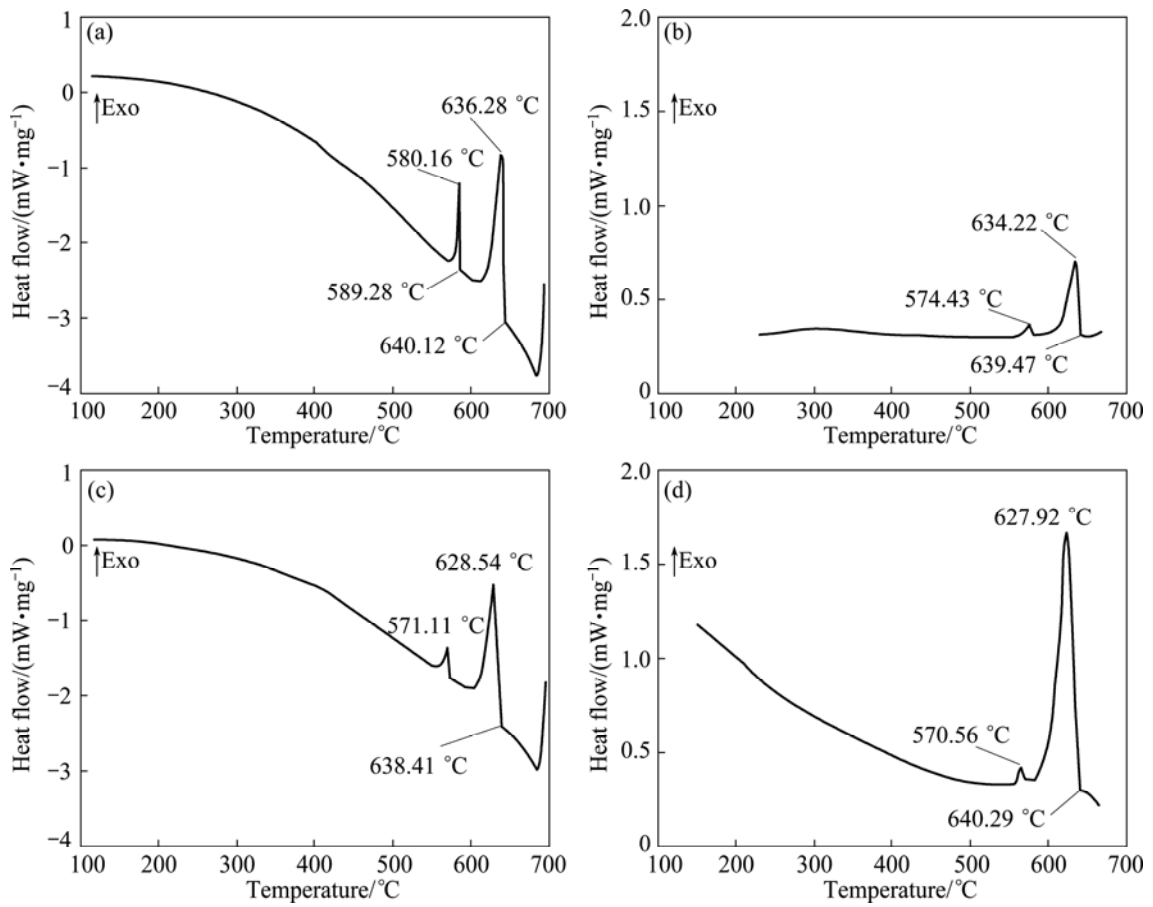


Fig. 1 DSC cooling curves of different as-cast alloys: (a) Mg-3Ce-1.2Mn-0.9Sc alloy; (b) Mg-3Ce-1.2Mn-0.9Sc-0.6Ca alloy; (c) Mg-4Y-1.2Mn-0.9Sc alloy; (d) Mg-4Y-1.2Mn-0.9Sc-0.6Ca alloy

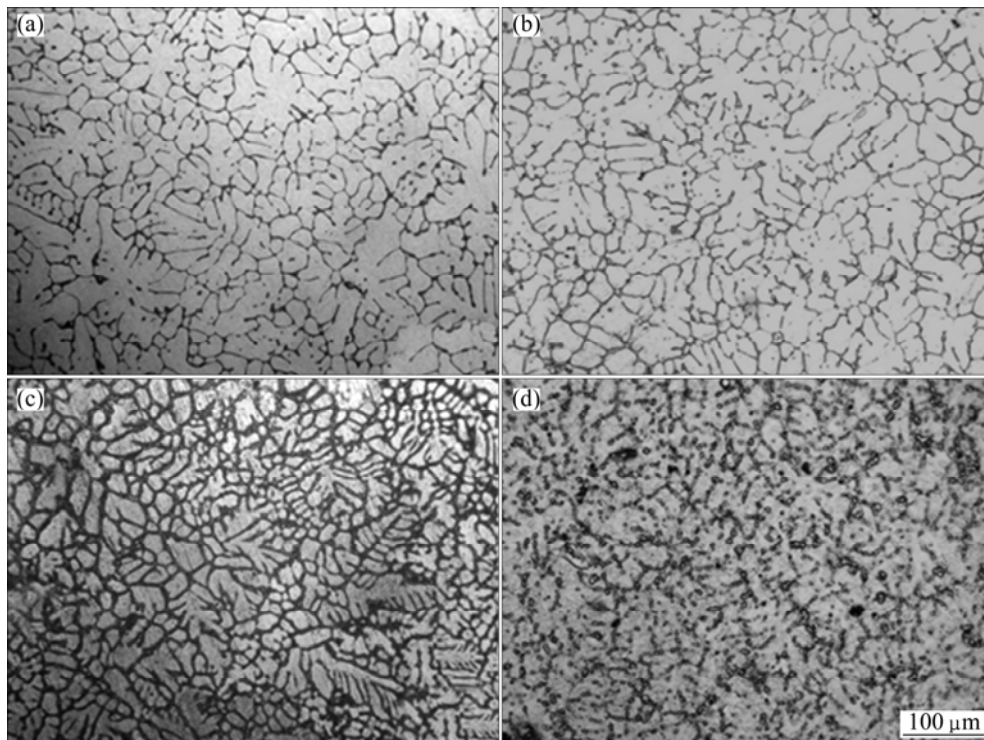


Fig. 2 Optical images of different as-cast alloys: (a) Mg-3Ce-1.2Mn-0.9Sc alloy; (b) Mg-3Ce-1.2Mn-0.9Sc-0.6Ca alloy; (c) Mg-4Y-1.2Mn-0.9Sc alloy; (d) Mg-4Y-1.2Mn-0.9Sc-0.6Ca alloy

display a dendrite configuration. Furthermore, it is found from Fig. 2 that the primary α -Mg phases in the Ca-containing alloys are relatively finer than those in the corresponding quaternary alloys, indicating that the addition of 0.6% Ca to the Mg–3Ce/4Y–1.2Mn–0.9Sc alloys possibly refines the grains of the two alloys. This is further confirmed from Fig. 3 which shows the optical images of the solutionized alloys. It is observed from Fig. 3 that the Ca-containing alloys exhibit relatively finer grains than their corresponding quaternary alloys. The average grain size before refining is 153 μm and 324 μm for the Mg–3Ce–1.2Mn–0.9Sc and Mg–4Y–1.2Mn–0.9Sc alloys, respectively, and after the addition of 0.6%Ca their average size is 87 μm and 216 μm for the Ca-containing Mg–3Ce–1.2Mn–0.9Sc and Mg–4Y–1.2Mn–0.9Sc alloys, respectively. Previous investigations reported that solute elements such as Zr, Ca and Si possess high growth restriction factors on Mg due to their strong segregating power [15,16]. At the same time, the X-ray mapping results of the Ca-containing Mg–3Ce/4Y–1.2Mn–0.9Sc alloys reveal that Ca element mainly distributes at the grain boundaries, as shown in Figs. 4 and 5. Therefore, it is preliminarily inferred that the grain growth restriction theory is possibly suitable for the grain refinement of the Ca-containing Mg–3Ce/4Y–1.2Mn–0.9Sc alloys. Based on the grain growth restriction theory, during the solidification of the Ca-containing alloys, Ca enrichment which induces a constitution undercooling at the solidification interface

front, possibly inhibits the growth of the grains thus leads to the grain refinement.

Figure 6 shows the SEM images of the as-cast Mg–3Ce–1.2Mn–0.9Sc alloys with and without Ca addition, and in Fig. 6 the second phases are identified by combining the XRD results with the EDS analysis (Table 2). As shown in Fig. 6, the Mg_{12}Ce and Mn_2Sc phases in the Mg–3Ce–1.2Mn–0.9Sc alloy without Ca addition exhibit particle-like shapes, and mainly distribute at the grain boundaries. However, after the addition of 0.6% Ca to the Mg–3Ce–1.2Mn–0.9Sc alloy, the morphology of the Mg_{12}Ce phases changes from the initial particle-like shapes to the continuous and/or quasi-continuous nets. At the same time, a small quantity of the Mg_{12}Ce phases with particle-like shapes are also observed in the Ca-containing Mg–3Ce–1.2Mn–0.9Sc alloy. In addition, it is further found that the Mg_{12}Ce phases in the Ca-containing Mg–3Ce–1.2Mn–0.9Sc alloy also mainly distribute at the grain boundaries, similar to the distribution of the Mg_{12}Ce phases in the Mg–3Ce–1.2Mn–0.9Sc alloy without Ca addition.

Figure 7 shows the SEM images of the Mg–4Y–1.2Mn–0.9Sc as-cast alloys with and without Ca addition, and in Fig. 7 the second phases are identified by combining the XRD results and the EDS analysis (Table 2). As shown in Fig. 7, the second phases in the alloys with and without Ca addition, such as Mg_{24}Y_5 , Mn_2Sc and Mn_{12}Y , mainly exhibit particle-like shapes and distribute both at the grain boundaries and inside

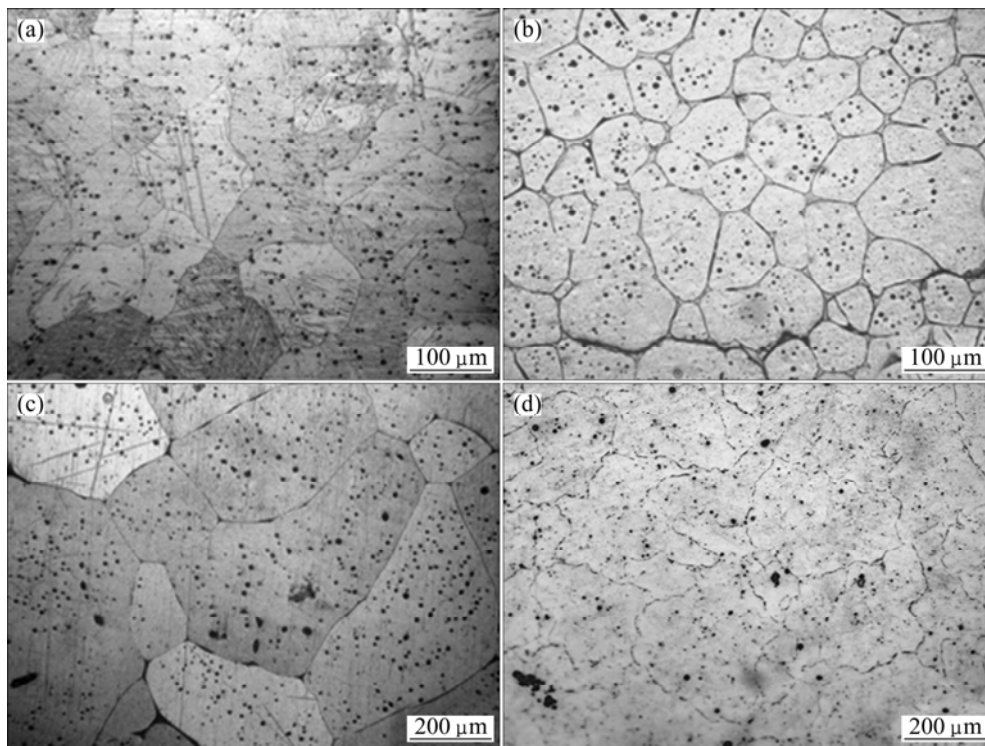


Fig. 3 Optical images of different solutionized alloys: (a) Mg–3Ce–1.2Mn–0.9Sc alloy; (b) Mg–3Ce–1.2Mn–0.9Sc–0.6Ca alloy; (c) Mg–4Y–1.2Mn–0.9Sc alloy; (d) Mg–4Y–1.2Mn–0.9Sc–0.6Ca alloy

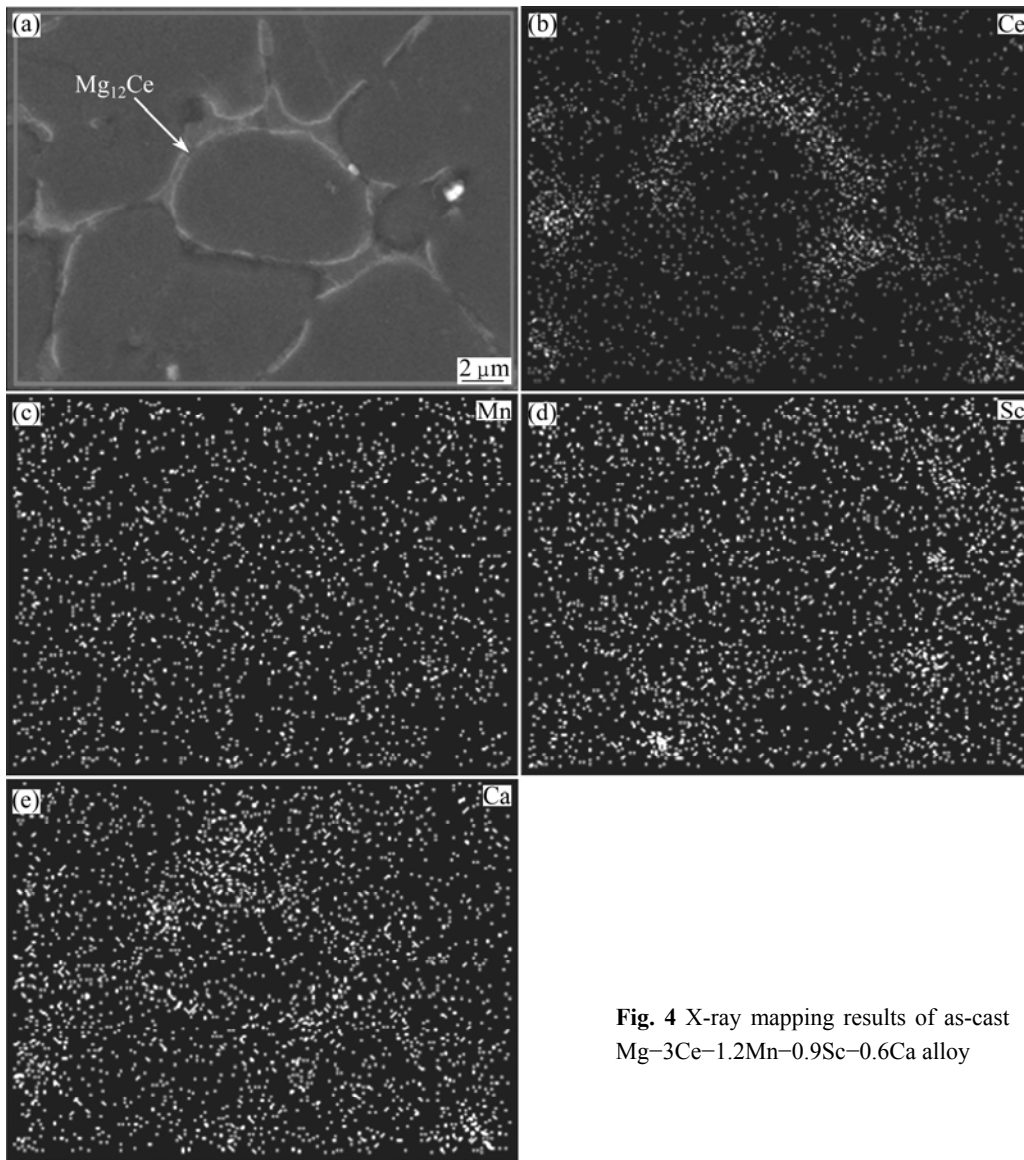


Fig. 4 X-ray mapping results of as-cast Mg-3Ce-1.2Mn-0.9Sc-0.6Ca alloy

Table 2 EDS results of as-cast alloys (mass fraction, %)

Position	Composition/%					
	Mg	Ce	Y	Mn	Sc	Ca
Fig. 6(b)-A	78.32	21.68	–	–	–	–
Fig. 6(b)-B	84.25	15.75	–	–	–	–
Fig. 6(b)-C	70.56	–	–	17.69	11.75	–
Fig. 6(d)-A	76.85	19.47	–	–	0.04	3.64
Fig. 6(d)-B	72.49	–	–	15.33	12.18	–
Fig. 7(b)-A	95.70	–	3.35	0.48	0.47	–
Fig. 7(b)-B	85.58	–	13.09	1.20	0.13	–
Fig. 7(b)-C	68.76	–	1.45	18.22	11.57	–
Fig. 7(b)-D	65.28	–	10.54	24.16	0.02	–
Fig. 7(d)-A	88.63	–	6.56	0.47	0.42	3.92
Fig. 7(d)-B	83.53	–	15.33	1.01	0.09	0.04
Fig. 7(d)-C	68.88	–	1.05	17.92	12.15	–
Fig. 7(d)-D	60.18	–	12.24	25.32	1.06	1.20

the grains. Furthermore, it is found that the Y-rich area for the Ca-containing Mg-4Y-1.2Mn-0.9Sc alloy is more obvious than that for the Mg-4Y-1.2Mn-0.9Sc alloy without Ca addition. In addition, as shown in Fig. 7, the amount of the second phases in the Mg-4Y-1.2Mn-0.9Sc alloy without Ca addition is relatively larger than that in the Ca-containing Mg-4Y-1.2Mn-0.9Sc alloy.

3.2 Effects of minor Ca on tensile properties

The tensile properties at room temperature and 300 °C for the as-cast alloys, including ultimate tensile strength (UTS), 0.2% yield strength (YS), and elongation (A), are listed in Table 3. It is observed that the Ca-containing Mg-3Ce/4Y-1.2Mn-0.9Sc alloys exhibit relatively higher tensile properties at the room temperature and 300 °C than their corresponding quaternary alloys, indicating that the addition of 0.6% Ca to the Mg-3Ce/4Y-1.2Mn-0.9Sc alloys is beneficial to the tensile properties of the two alloys. Obviously, the

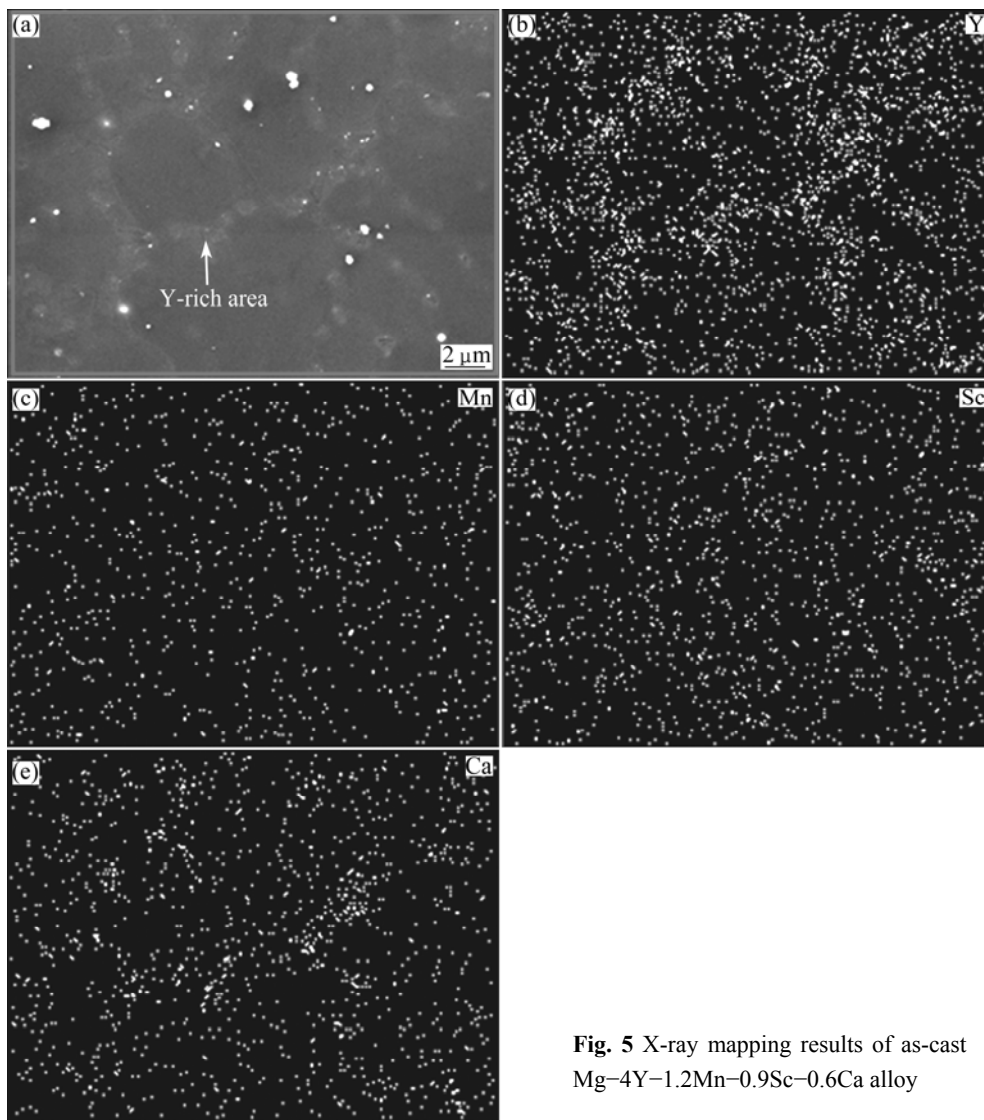


Fig. 5 X-ray mapping results of as-cast Mg-4Y-1.2Mn-0.9Sc-0.6Ca alloy

effects of minor Ca on the tensile properties of the Mg-3Ce/4Y-1.2Mn-0.9Sc alloys can be easily explained by the grain refinement. In addition, the effects of minor Ca on the tensile properties of the Mg-3Ce/4Y-1.2Mn-0.9Sc alloys can be further confirmed from Fig. 8, which shows the SEM images of tensile fractographs for the as-cast alloys failed in the tensile tests at room temperature. As shown in Fig. 8, a number of cleavage planes and steps are present, and some river patterns can also be observed in the tensile fracture surfaces of the experimental alloys, indicating that all the tensile fracture surfaces have mixed characteristics of cleavage and quasi-cleavage fractures. Obviously, the addition of 0.6% Ca to Mg-3Ce/4Y-1.2Mn-0.9Sc alloys does not significantly change the fracture mode of the two alloys. However, some relatively obvious lacerated ridges are observed in the tensile fracture surfaces of the Mg-3Ce/4Y-1.2Mn-0.9Sc alloys without Ca addition (Figs. 8(a) and (c)),

which is consistent with the relatively poor tensile properties of the two alloys.

3.3 Effects of minor Ca on creep properties

The creep properties at 300 °C and 30 MPa for 100 h for the as-cast alloys, including total creep strain and minimum creep rate, are listed in Table 4. As shown in Table 4, the creep properties of the Ca-containing Mg-3Ce-1.2Mn-0.9Sc alloy are obviously higher than those of the corresponding quaternary alloy, indicating that the addition of 0.6% Ca to the Mg-3Ce-1.2Mn-0.9Sc alloy is beneficial to the creep properties. However, the opposite results for the creep properties of the Ca-containing Mg-4Y-1.2Mn-0.9Sc alloy are observed as compared with the Mg-4Y-1.2Mn-0.9Sc alloy without Ca addition. Figure 9 shows the SEM images of the solutionized Mg-3Ce-1.2Mn-0.9Sc alloys with and without Ca addition. It is observed from Fig. 9 that a majority of the Mg₁₂Ce phases in the quaternary alloy

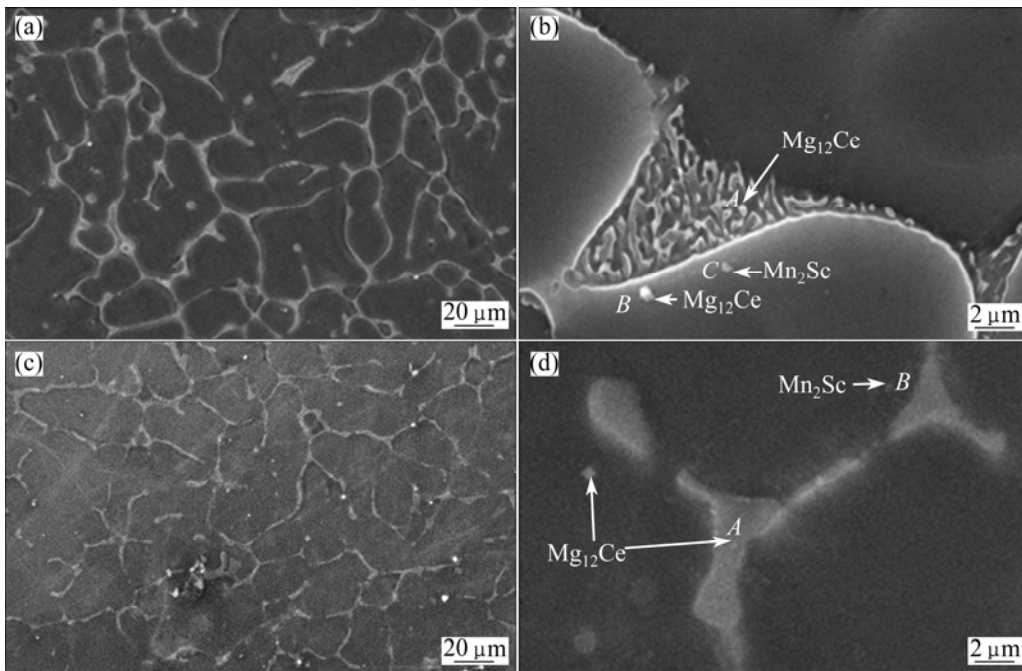


Fig. 6 SEM images of Ce-containing as-cast alloys: (a, b) Mg–3Ce–1.2Mn–0.9Sc alloy; (c, d) Mg–3Ce–1.2Mn–0.9Sc–0.6Ca alloy

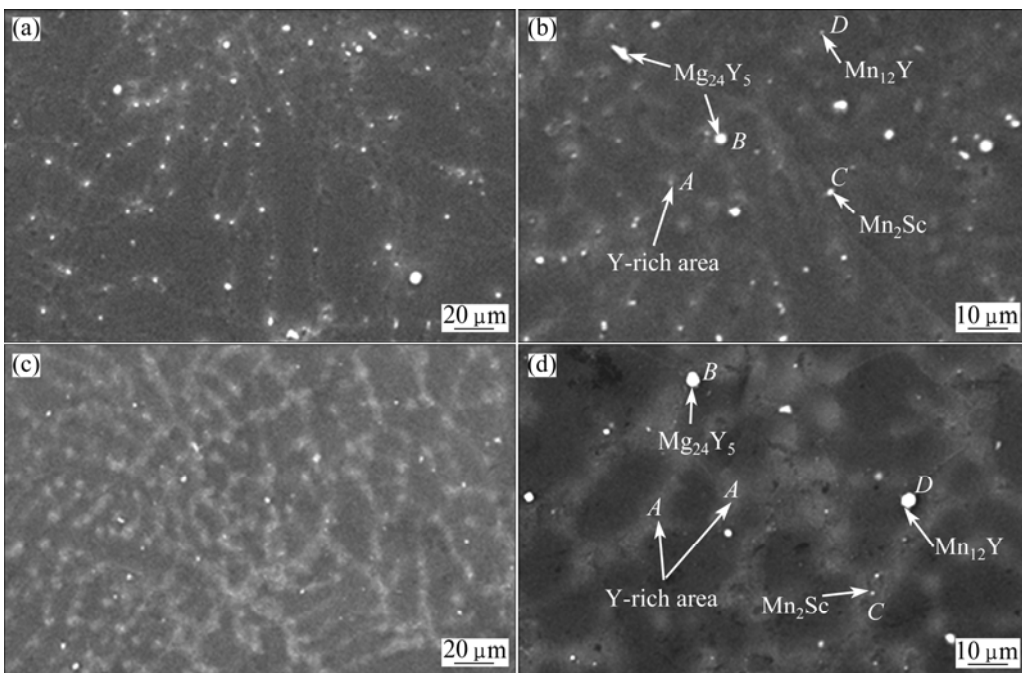


Fig. 7 SEM images of Y-containing as-cast alloys: (a, b) Mg–4Y–1.2Mn–0.9Sc alloy; (c, d) Mg–4Y–1.2Mn–0.9Sc–0.6Ca alloy

have dissolved into the matrix after solid solution treatment at 520 °C for 12 h. However, under the same heat-treated conditions, the remnant $Mg_{12}Ce$ phases in the Ca-containing Mg–3Ce–1.2Mn–0.9Sc alloy seem to be more than that in the quaternary alloy. Obviously, the addition of 0.6% Ca to the Mg–3Ce–1.2Mn–0.9Sc alloy is beneficial to the thermal stability of the $Mg_{12}Ce$ phases in the alloy. According to the EDS results listed in Table 2, it is found that, for the Ca-containing Mg–3Ce–

1.2Mn–0.9Sc alloy, Ca dissolves into the $Mg_{12}Ce$ compound. Based on the above results and combined with the results that Ca addition to Mg–Al alloys results in higher thermal stability of the $Mg_{17}Al_{12}$ phase [17], it is preliminarily believed that the higher thermal stability of the $Mg_{12}Ce$ phases in Ca-containing Mg–3Ce–1.2Mn–0.9Sc alloy than in the quaternary alloy is possibly related to the dissolving of Ca in the $Mg_{12}Ce$ phase. Since the creep resistance properties of

Table 3 Tensile properties at room temperature and 300 °C for as-cast alloys

Alloys	Room temperature			300 °C		
	UTS/MPa	YS/MPa	A/%	UTS/MPa	YS/MPa	A/%
Mg–3Ce–1.2Mn–0.9Sc	161 (3.1)	133 (1.9)	3.1 (0.25)	108 (2.1)	90 (1.8)	16.0 (0.89)
Mg–3Ce–1.2Mn–0.9Sc–0.6Ca	174 (2.4)	150 (1.5)	3.6 (0.31)	113 (2.7)	102 (2.5)	18.1 (1.03)
Mg–4Y–1.2Mn–0.9Sc	194 (4.2)	176 (3.6)	3.6 (0.27)	129 (3.1)	112 (2.9)	17.0 (0.96)
Mg–4Y–1.2Mn–0.9Sc–0.6Ca	215 (4.2)	183 (3.9)	4.5 (0.12)	130 (1.6)	118 (3.2)	19.8 (0.65)

Data in the bracket are standard errors

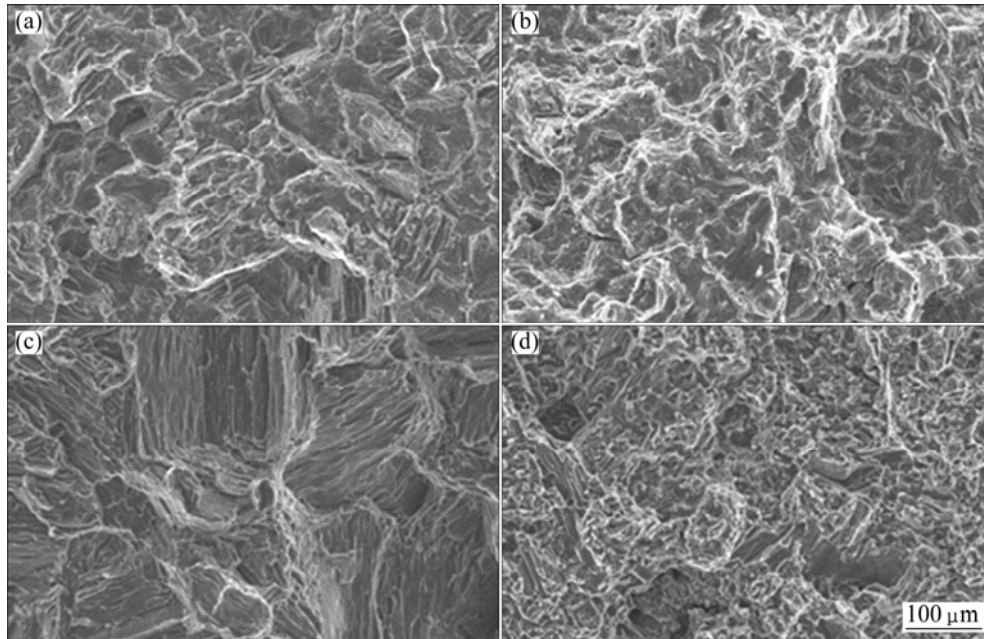


Fig. 8 SEM images of tensile fractographs for different as-cast alloys tested at room temperature: (a) Mg–3Ce–1.2Mn–0.9Sc alloy; (b) Mg–3Ce–1.2Mn–0.9Sc–0.6Ca alloy; (c) Mg–4Y–1.2Mn–0.9Sc alloy; (d) Mg–4Y–1.2Mn–0.9Sc–0.6Ca alloy

magnesium alloys are mainly related to the structure stability at high temperatures [18], it is inferred that the improvement in the creep properties for the Ca-containing Mg–3Ce–1.2Mn–0.9Sc alloy is possibly related to the effect of Ca addition on the thermal stability of the Mg₁₂Ce phase.

Figure 10 shows the SEM images of the solutionized Mg–4Y–1.2Mn–0.9Sc alloys with and without Ca addition. It is observed from Fig. 10 that, after being solutionized at 520 °C for 12 h, the amount of the remnant secondary phases in the Ca-containing Mg–4Y–1.2Mn–0.9Sc alloy seems to be smaller than that in the quaternary alloy, which is possibly related to the difference in the initial as-cast microstructures of the two alloys (see Fig. 7). Obviously, the effects of minor Ca on the creep properties of the Mg–4Y–1.2Mn–0.9Sc alloy is consistent with the difference in the microstructures of Mg–4Y–1.2Mn–0.9Sc alloys with and without Ca addition.

3.4 Discussion

The above results indicate that minor Ca to the

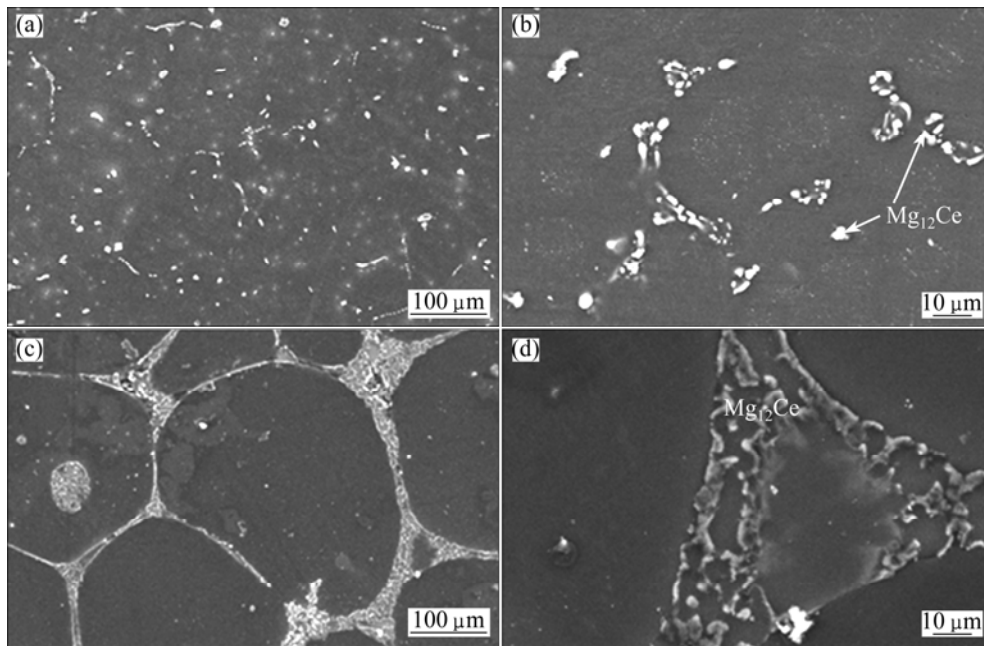
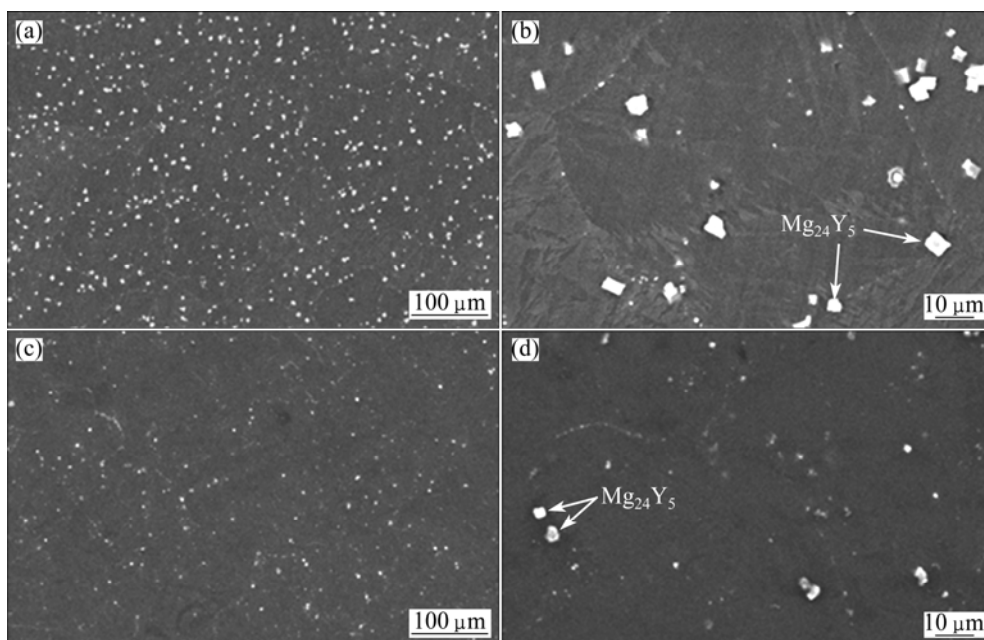
Mg–3Ce–1.2Mn–0.9Sc and Mg–4Y–1.2Mn–0.9Sc alloys can refine the grains of the two alloys. At the same time, the tensile properties of the Mg–3Ce/4Y–1.2Mn–0.9Sc alloys with minor Ca addition are effectively improved. In addition, minor Ca can also improve the creep properties of the Mg–3Ce–1.2Mn–0.9Sc alloy but is not beneficial to the creep properties of the Mg–4Y–1.2Mn–0.9Sc alloy. Since the mechanisms for the grain refinement and the improvement in the tensile properties for the Mg–3Ce/4Y–1.2Mn–0.9Sc alloys with minor Ca addition have been explained in the above sections, the following discussions mainly focus on the different effects of minor Ca on the creep properties of the Mg–3Ce–1.2Mn–0.9Sc and Mg–4Y–1.2Mn–0.9Sc alloys. Previous investigations from JUN et al [12] indicated that the additions of 0.5% and 1.0% Ca to the Mg–1.5Nd–1.0RE alloy result in a similar effects on the creep properties as the addition of 0.6% Ca to the Mg–3Ce–1.2Mn–0.9Sc alloy. At the same time, similar to the above results that the addition of 0.6% Ca to the Mg–4Y–1.2Mn–0.9Sc alloy causes the amount of the secondary phases to decrease thus leads to decrease the

Table 4 Creep properties of as-cast alloys at 300 °C and 30 MPa for 100 h

Alloy	Total creep strain/%	Minimum creep rate/(10^{-9} s^{-1})
Mg-3Ce-1.2Mn-0.9Sc	0.457 (0.10)	12.70 (0.39)
Mg-3Ce-1.2Mn-0.9Sc-0.6Ca	0.226 (0.05)	6.28 (0.42)
Mg-4Y-1.2Mn-0.9Sc	0.343 (0.11)	9.52 (0.21)
Mg-4Y-1.2Mn-0.9Sc-0.6Ca	0.412 (0.09)	11.40 (0.46)

Data in the bracket are standard errors

creep properties, YANG et al [19] found that, after the addition of 0.3% Ca to Mg-5Gd-1.2Mn-0.4Sc alloy, the amount of the secondary phases in the alloy is also decreased. It is well known that, although Ce, Nd, Y and Gd elements have approximate atomic radius (Ce: 0.183 nm; Nd: 0.182 nm; Y: 0.182 nm and Gd: 0.178 nm), the solid solubilities of the four elements in Mg are different [20]. The solid solubilities of Ce and Nd in Mg are relatively low (1.6% Ce and 3.6% Nd), oppositely, the solid solubilities of Y and Gd in Mg are very high

**Fig. 9** SEM images of different Ce-containing solutionized alloys: (a, b) Mg-3Ce-1.2Mn-0.9Sc alloy; (c, d) Mg-3Ce-1.2Mn-0.9Sc-0.6Ca alloy**Fig. 10** SEM images of different Y-containing solutionized alloys: (a, b) Mg-4Y-1.2Mn-0.9Sc alloy; (c, d) Mg-4Y-1.2Mn-0.9Sc-0.6Ca alloy

(12.6% Y and 23.5% Gd). Therefore, it is preliminarily inferred that the different effects of minor Ca on the creep properties of Mg–3Ce–1.2Mn–0.9Sc and Mg–4Y–1.2Mn–0.9Sc alloys are possibly related to the difference in the solid solubilities of Ce and Y in Mg, and the simple analysis is given as follows. During the solidification process of the Ca-containing Mg–3Ce/4Y–1.2Mn–0.9Sc alloys, Ca element is rich in the solid-liquid interface due to the very low solid solubility of Ca in Mg (0.73%). Then, the diffusion of Ce and Y atoms riched in the solid-liquid interface is hindered because Ca atom has larger atomic radius than Ce and Y atoms (Ca: 0.197 nm; Ce: 0.183 nm and Y: 0.182 nm), which results in the more obvious gather at the grain boundaries and smaller amount inside the grains for Ce and Y atoms as compared with the Mg–3Ce/4Y–1.2Mn–0.9Sc alloys without Ca addition. Accordingly, the following different results for the Ca-containing Mg–3Ce–1.2Mn–0.9Sc and Mg–4Y–1.2Mn–0.9Sc alloys arise due to the difference in the solid solubilities of Ce and Y in Mg. 1) For the Ca-containing Mg–3Ce–1.2Mn–0.9Sc alloy, the morphology of the Mg₁₂Ce phase at grain boundaries is changed from the initial particle-like shapes to the continuous and/or quasi-continuous blocks (see Fig. 6). At the same time, Ca also dissolves into the Mg₁₂Ce compound, which results in an increase in the thermal stability for the Mg₁₂Ce phases in the Ca-containing Mg–3Ce–1.2Mn–0.9Sc alloy (see Fig. 9). As a result, the creep properties of the Ca-containing Mg–3Ce–1.2Mn–0.9Sc alloy are increased. 2) For the Ca-containing Mg–4Y–1.2Mn–0.9Sc alloy, the obvious Y-rich area is formed at grain boundaries and the amount of the secondary phases decreases (see Fig. 7). Accordingly, the creep properties of the Ca-containing Mg–4Y–1.2Mn–0.9Sc alloy are decreased. In spite of the above analysis, the reason for the different effects of minor Ca on the creep properties of the Mg–3Ce–1.2Mn–0.9Sc and Mg–4Y–1.2Mn–0.9Sc alloys, is not completely clear because some phenomena still are not explained. For example, although the addition of 0.6% Ca to the Mg–4Y–1.2Mn–0.9Sc alloy causes the obvious gather of Y atom in the solid-liquid interface front, the amount of the second phases at the grain boundaries for the Ca-containing Mg–4Y–1.2Mn–0.9Sc alloy does not increase and only the Y-rich area is obviously formed (see Fig. 7). Therefore, further investigation needs to be considered.

4 Conclusions

1) The addition of 0.6% Ca to the Mg–3Ce–1.2Mn–0.9Sc and Mg–4Y–1.2Mn–0.9Sc alloys does not cause the formation of any new phases in the two alloys. However, the grains of both the Ca-containing

Mg–3Ce–1.2Mn–0.9Sc and Mg–4Y–1.2Mn–0.9Sc alloys are refined.

2) The addition of 0.6% Ca to the Mg–3Ce–1.2Mn–0.9Sc and Mg–4Y–1.2Mn–0.9Sc alloys can effectively improve the tensile properties of the two alloys. In addition, the addition of 0.6% Ca can also improve the creep properties of the Mg–3Ce–1.2Mn–0.9Sc alloy but is not beneficial to the creep properties of the Mg–4Y–1.2Mn–0.9Sc alloy. The different effects of minor Ca on the creep properties of the Mg–3Ce–1.2Mn–0.9Sc and Mg–4Y–1.2Mn–0.9Sc alloys are possibly related to the difference in the solid solubilities of Ce and Y in Mg.

References

- [1] MORDIKE B L, STULIKOVA I, SMOLA B. Mechanisms of creep deformation in Mg–Sc-based alloys [J]. *Metallurgical and Materials Transactions A*, 2005, 36(7): 1729–1736.
- [2] BUCH F V, LIETZAU J, MORDIKE B L, PISCH A, SCHMID-FETZER R. Development of Mg–Sc–Mn alloys [J]. *Materials Science and Engineering A*, 1999, 263(1): 1–7.
- [3] MORDIKE B L. Development of highly creep resistant magnesium alloys [J]. *Journal of Materials Processing Technology*, 2001, 117(3): 391–394.
- [4] STULIKOVA I, SMOLA B, BUCH F V, MORDIKE B L. Mechanical properties and creep of Mg–rare earth–Sc–Mn squeeze cast alloys [J]. *Materialwissenschaft und Werkstofftechnik*, 2003, 34(1): 102–108.
- [5] SMOLA B, STULIKOVA I, PELCOVA J, BUCH F V, MORDIKE B L. Microstructure and phase changes due to heat treatment of squeeze cast Mg–Sc–(Ce)–Mn alloys [J]. *Physica Status Solidi (A)*, 2002, 191(1): 305–316.
- [6] SMOLA B, STULIKOVA I, BUCH F V, MORDIKE B L. Structural aspects of high performance Mg alloys design [J]. *Materials Science and Engineering A*, 2002, 324(1–2): 113–117.
- [7] SMOLA B, STULIKOVA I, PELCOVA J. Significance of stable and metastable phases in high temperature creep resistant magnesium–rare earth base alloys [J]. *Journal of Alloys and Compounds*, 2004, 378(1–2): 196–201.
- [8] PAN F S, YANG M B, SHEN J, WU L. Effects of minor Zr and Sr on as-cast microstructure and mechanical properties of Mg–3Ce–1.2Mn–0.9Sc (wt.%) magnesium alloy [J]. *Materials Science and Engineering A*, 2011, 528(13–14): 4292–4299.
- [9] YANG M B, PAN F S, ZHU Y, SHEN J. Effects of small additions of Zr and Sr on as cast microstructure and tensile properties of Mg–4Y–1.2Mn–0.9Sc (wt.%) alloy [J]. *Materials Science and Technology*, 2012, 28(2): 144–150.
- [10] YANG M B, CHENG L, PAN F S. Comparison about effects of Ce, Sn and Gd additions on as-cast microstructure and mechanical properties of Mg–3.8Zn–2.2Ca (wt.%) magnesium alloy [J]. *Journal of Materials Science*, 2009, 44(17): 4577–4586.
- [11] JUN J H, PARK B K, KIM J M, KIM K T, JUNG W J. Effects of Ca addition on microstructure and mechanical properties of Mg–RE–Zn casting alloys [J]. *Materials Science Forum*, 2005, 488–489: 107–110.
- [12] JUN J H, PARK B K, KIM J M, KIM K T, JUNG W J. Microstructure and tensile creep behavior of Mg–Nd–RE–Ca casting alloys [J]. *Key Engineering Materials*, 2007, 345–346: 557–560.
- [13] ZHANG J S, SUN Y, CHENG W L, QUE Z P, LI Y M. The effect of Ca addition on microstructures and mechanical properties of Mg–RE

- based alloys [J]. Journal of Alloys and Compounds, 2013, 554: 110–114.
- [14] YANG Ming-bo, QIN Cai-yuan, PAN Fu-sheng. Effects of heat treatment on microstructure and mechanical properties of Mg–3Sn–1Mn magnesium alloy [J]. Transactions of Nonferrous Metals Society of China, 2011, 21(10): 2168–2174.
- [15] LEE Y C, DAHLE A K, STJOHN D H. The role of solute in grain refinement of magnesium [J]. Metallurgical and Materials Transactions A, 2000, 31(11): 2895–2906.
- [16] STJOHN D H, QIAN M, EASTON M A, CAO P, HILDEBRAND Z. Grain refinement of magnesium alloys [J]. Metallurgical and Materials Transactions A, 2005, 36 (7): 1669–1679.
- [17] DU W W, SUN YS, MIN X G, XUE F, ZHU M, WU D Y. Microstructure and mechanical properties of Mg–Al based alloy with calcium and rare earth additions [J]. Materials Science and Engineering A, 2003, 356(1–2): 1–7.
- [18] ZHU S M, MORDIKE B L, NIE J F. Creep properties of a Mg–Al–Ca alloy produced by different casting technologies [J]. Materials Science and Engineering A, 2008, 483–484: 583–586.
- [19] YANG M B, LI H L, CHENG R J, PAN F S, HU H J. Comparison about effects of minor Zr, Sr and Ca additions on microstructure and tensile properties of Mg–5Gd–1.2Mn–0.4Sc (wt.%) magnesium alloy [J]. Materials Science and Engineering A, 2012, 545: 201–208.
- [20] ZHANG J H, LIU H F, SUN W, LU F Y, TANG D X, MENG J. Influence of structure and ionic radius on solubility limit in Mg–RE systems [J]. Materials Science Forum, 2007, 561–565: 143–146.

少量 Ca 对 Mg–3Ce–1.2Mn–0.9Sc 和 Mg–4Y–1.2Mn–0.9Sc 镁合金铸态组织和力学性能的影响

杨明波^{1,2,3}, 段成宇², 吴德勇², 潘复生³

1. 重庆理工大学 汽车零部件制造及检测技术教育部重点实验室, 重庆 400054;
2. 重庆理工大学 材料科学与工程学院, 重庆 400054;
3. 重庆大学 国家镁合金工程材料研究中心, 重庆 400030

摘要: 通过光学显微镜、电子显微镜、差热分析以及抗拉和蠕变性能测试等手段, 研究和比较 0.6% Ca(质量分数)添加对 Mg–3Ce–1.2Mn–0.9Sc 和 Mg–4Y–1.2Mn–0.9Sc 镁合金铸态组织和力学性能的影响。结果表明: 添加 0.6% Ca 能细化 Mg–3Ce–1.2Mn–0.9Sc 和 Mg–4Y–1.2Mn–0.9Sc 合金的晶粒。同时, 添加 0.6% Ca 也能有效改善 Mg–3Ce–1.2Mn–0.9Sc 和 Mg–4Y–1.2Mn–0.9Sc 合金的抗拉性能。此外, 添加 0.6% Ca 能改善 Mg–3Ce–1.2Mn–0.9Sc 合金的蠕变性能, 但对 Mg–4Y–1.2Mn–0.9Sc 合金的蠕变性能是不利的。少量 Ca 对 Mg–3Ce–1.2Mn–0.9Sc 和 Mg–4Y–1.2Mn–0.9Sc 合金蠕变性能的不同影响可能与 Ce 和 Y 在 Mg 中的固溶度存在差异有关。

关键词: 镁合金; Mg–RE–Mn–Sc 合金; Ca 添加

(Edited by Chao WANG)